Available online at www.sciencedirect.com

ScienceDirect

Ceramics International 39 (2013) 9651–9658

CERAMICS INTERNATIONAL

www.elsevier.com/locate/ceramint

Preparation and characterization of copper oxide particles incorporated polyurethane composite nanofibers by electrospinning

R. Nirmala[a,*], Kyung Soo Jeon[a], Baek Ho Lim[a], R. Navamathavan[b],
Hak Yong Kim[a,*]

[a]Department of Organic Materials and Fiber Engineering, Chonbuk National University, Jeonju 561-756, South Korea
[b]School of Advanced Materials Engineering, Chonbuk National University, Jeonju 561-756, South Korea

Received 23 April 2013; received in revised form 20 May 2013; accepted 20 May 2013
Available online 30 May 2013

Abstract

In this paper, we demonstrate the preparation of copper oxide (CuO) particles incorporated polyurethane (PU) composite nanofibers by using electrospinning. Two step processes were adopted to incorporate the CuO particles in PU nanofibers. In the first step, the cupric acetate was added to poly(vinyl alcohol) to obtain a thin film by wet casting. Then the thin film was calcined at 500 °C and ground to prepare the CuO particles. In the second step, these CuO particles were incorporated in the PU to obtain composite nanofibers. Different types of nanofiber mats were prepared by varying the concentration of CuO particles. The surface morphology, structure, bonding configuration, thermal, optical and electrical properties of the resultant nanofibers were characterized by means of scanning electron microscopy (SEM), X-ray diffraction (XRD), Fourier transform infrared spectroscopy (FT-IR), UV–vis (ultraviolet visible) spectroscopy, thermogravimetric, photoluminescence and current–voltage analysis. The electrical conductivities of the PU/CuO composite nanofibers were markedly improved than that of pristine PU nanofibers. The improvement of electrical properties is attributed to the better carrier transport in the composite nanofibers.

Keywords: A. Electrospinning; C. Electrical properties; D. CuO particles; D. Polyurethane

1. Introduction

One-dimensional (1D) nanomaterials have attracted growing attention due to their unique physical traits including their electronic, magnetic, optical, and mechanical properties [1–4]. Various strategies have been proposed for obtaining these materials. A variety of nano-scale materials with different morphologies have been synthesized by using various methods including chemical vapor deposition, arc discharge, laser ablation, electrospinning and template based physical vapor transport [5–11]. Among them, electrospinning is a simple and sophisticated technique for producing nanofibers. The main advantage of electrospinning is the relatively quick and simple way to fabricate a variety of materials into nanofibrous structure. During last decade electrospinning of polymers has become highly recognized method for obtaining polymer nanofibers with diameters down to a few nanometers and of a broad range of complex architectures of nanofibers and nonwovens [12–15]. Polymeric nanofibers exhibit unusual properties due to their very small diameter, which leads to high surface area, high aspect ratio, and better mechanical properties. These remarkable properties underlie the substantial interests in these materials for industrial, biomedical, and electronic applications.

In the past few years, a wide range of synthetic and natural polymers in pure or blend solutions have been electrospun to form nanofibers. In particular, polyurethane (PU) is a thermoplastic resilient elastomer of significant industrial importance which possesses a wide range of desirable properties such as elastomeric, resistant to abrasion, and excellent hydrolytic stability [16–18]. Numerous studies on the electrospinning of PU have been conducted. Electrospun PU nanofiber mats exhibit good mechanical properties and have a wide variety of potential application in high-performance air filters, protective

---

[*] Corresponding authors. Tel.: +82 63 270 2351; fax: +82 63 270 4249.
E-mail addresses: nirmalmathu@gmail.com (R. Nirmala), khy@jbnu.ac.kr (H.Y. Kim).

0272-8842/$ - see front matter © 2013 Elsevier Ltd and Techna Group S.r.l. All rights reserved.
http://dx.doi.org/10.1016/j.ceramint.2013.05.087

textiles, wound dressing materials and sensors [19–24]. Due to these merits, PU nanofibers have been found to be a very promising material of interest. The properties of PU can be adjusted desirably based on the requirements. Metal oxide containing PU nanofibers are of great interest in many technological applications. Such kinds of composite nanofiber materials can have much improved properties in terms of thermal stability, flexibility and solubility with that of the pristine PU nanofibers.

The oxides of transition metals are of important class of semiconductors, which can be utilized for variety of applications in magnetic storage media, solar energy transformation, electronics and catalysis [25–28]. Among the oxides of transition metals, copper oxide (CuO) nanoparticles are of special interest because of their efficiency as nanofluids in heat transfer application. CuO is a semiconducting compound with a narrow band gap and also used for photoconductive and photothermal applications [29]. Much effort has been devoted to synthesizing unique CuO nanostructures, such as, rods, wires, ribbons, cubes, spheres and dandelions [30–32]. The gas sensing responses of oxide materials can be improved with increasing surface-area-to-volume ratio. Therefore, the development of oxide materials with 1D geometry is highly desirable.

Nanofiber structures are investigated for their electrical properties and device characterizations. The electrical conductance is a fundamental quantity encountered in every study of electrical transport phenomena in nanostructured materials. Polymer nanofibers can be more readily applicable if their electrical conductivities were enhanced. The electrical conductivities of PU nanofibers can be significantly improved by adding metal oxide nanoparticles with high electric conductivities. The electrical property is known to influence the characteristics of the device and its stability under an electric field.

In this study, we prepared CuO nanoparticles incorporated PU composite nanofibers by using the electrospinning process. Different types of PU/CuO composite nanofibers were electrospun by varying the concentration of CuO nanoparticles. The prepared PU/CuO composite nanofibers were analyzed by scanning electron microscopy (SEM), energy dispersive X-ray analysis (EDX), X-ray diffraction (XRD), Fourier transform (FT-IR), thermogravimetric analysis (TGA) UV–vis, photoluminescence (PL) and current–voltage (*I*–*V*) measurements.

2. Experimental

2.1. Materials

Poly(vinyl alcohol) (PVA) solution (number averaged molecular weight (Mw)=85,000–124,000 g/mol, degree of hydrolysis=87–89%, Aldrich Co., USA) and copper acetate (Aldrich Co., USA) were used to prepare CuO particles. Polyurethane (PU, Mw=110,000) was purchased from Cardio Tech, Japan. Tetrahydrofuran (THF) and NN-dimethylformamide (DMF) (analytical grade, Showa, Japan) were used as solvents without further purification. PU solution with 10 wt% was prepared by dissolving in THF and DMF (1:1). All the above chemical reagents used were of analytical grade and used without further purification.

2.2. Preparation of CuO particles

Initially, 0.4 g cupric acetate was added in 1 g of water and then slowly mixed into 7.6 g of PVA aqueous solution (10 wt %). The solution was kept under vigorous magnetic stirring until to obtain a viscous gel. Then the viscous gel was gently poured in the Petri dish to obtain thin film by wet casting. The thin film was calcined at500 °C in air ambient for 5 h to remove the organic constituents of PVA and convert the precursor into pure CuO particles. The resultant product was further ground to reduce the particle size.

2.3. Electrospinning

The PU polymer solution for electrospinning was prepared by dissolving 10 wt% of PU in 85% DMF and THF solvent in ratio of 1:1. Later 1, 5 and 10 wt% of the CuO particles were mixed in the polymer solution to make the composite nanofibers. Then the polymer solution containing the CuO particle was loaded into a 5 ml plastic syringe equipped with a polystyrene micro-tip (0.3 mm inner diameter and 10 mm length), which was connected to a high-voltage power supply (CPS-60 K02V1, Chungpa EMT, South Korea). Electrospinning was performed at a voltage of 17 kV. A grounded iron drum was rotated at a constant speed by a DC motor to collect the developing nanofibers, which was kept at a distance of 15 cm from the micro-tip. All experiments were conducted at room temperature. Later, the electrospun PU mats were detached from the collector and vacuum dried for 24 h. The resultant nanofiber mats were utilized for the further characterizations.

2.4. Characterizations

The morphology of the electrospun PU and PU/CuO nanofibers were observed by using scanning electron microscopy (SEM, Hitachi S-7400, Hitachi, Japan). Elemental composition analysis of the composite nanofibers was carried out by using a SEM equipped with an energy dispersive X-ray (EDX) spectrometer. Structural characterization was carried out by X-ray diffraction (XRD) in a Rigaku X-ray diffractometer operated with Cu Kα radiation (λ=1.540 Å). The bonding configurations of the samples were characterized by means of Fourier transform infrared (FT-IR). Thermogravimetric analysis (TGA, Perkin-Elmer, USA) was carried out for the samples under nitrogen ambient with a flow rate of 20 mL/min. The samples were heated from 30 to 800 °C at a rate of 10 °C/min. The UV–vis spectra were measured in the range of 200–800 nm by using a UV–vis spectrometer (Lambda 900, Perkin-Elmer, USA). The optical property of Pu/CuO composite nanofibers was characterized by photoluminescence (PL) analysis using a 325 nm He–Cd laser. To study the electrical properties, several circular silver electrodes with a diameter of about 500 μm at a distance of 0.5 mm were made on the $1 \times 1\ \mathrm{cm}^2$ of composite nanofibers. Silver metal contacts were made on the nanofiber mat to have good ohmic contact. Then the current–voltage (*I*–*V*) characteristic was measured for the composite nanofibers by using a semiconductor parameter analyzer (4200-SCS, Keithley).

3. Results and discussion

Fig. 1 shows the morphology of the electrospun nanofibers. Fig. 1(a) shows the low and high magnification SEM image of the pristine PU nanofibers. The pristine PU nanofibers exhibited smooth surface and bead-free nature. The diameters of the nanofibers are in the range of 100–300 nm along their lengths. Fig. 1(b)–(d) shows the low and high magnification SEM image of PU/CuO composite nanofibers with CuO particles concentration of 1%, 5% and 10%, respectively. Significant morphological difference can be observed among pristine and

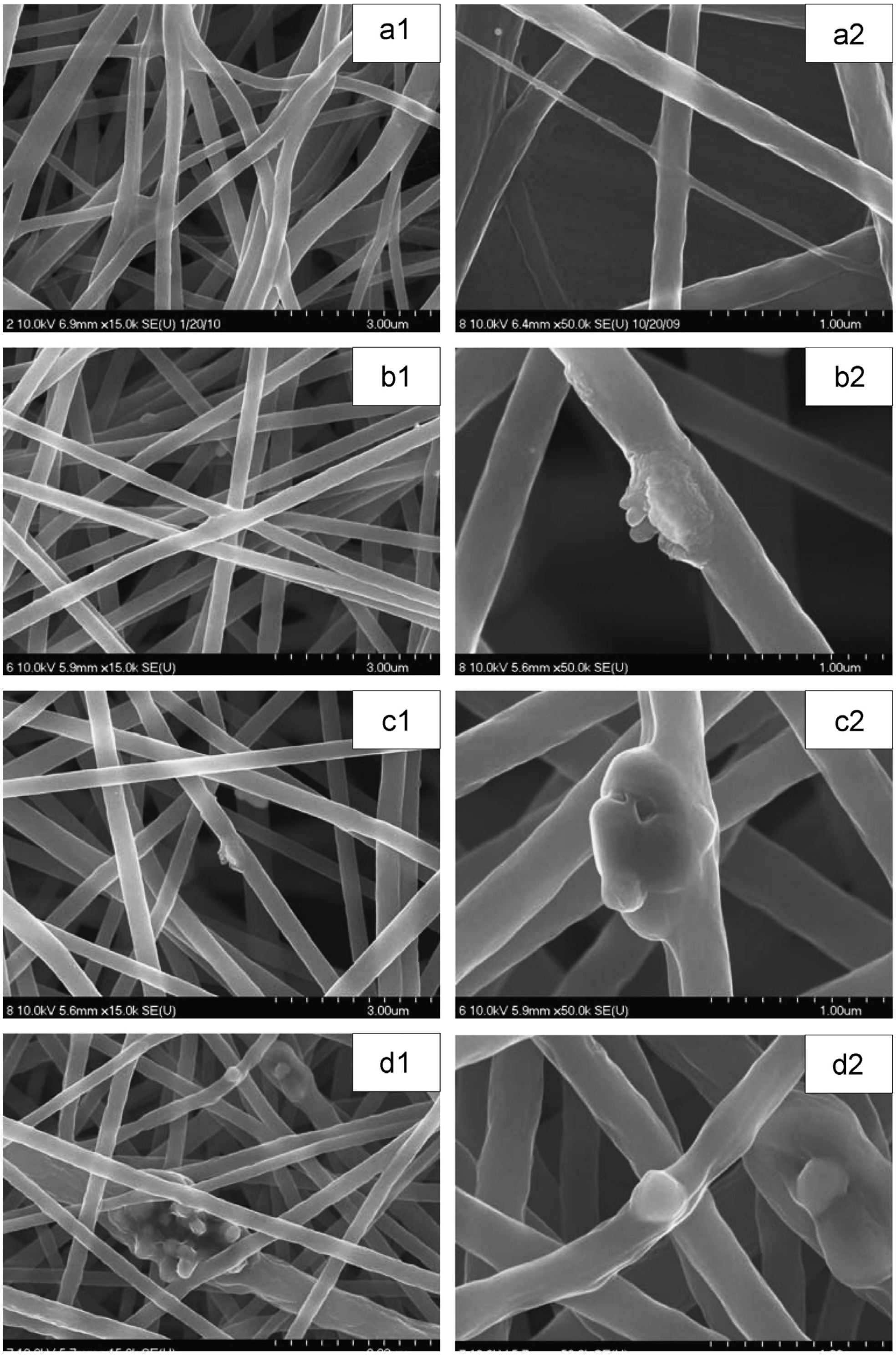

Fig. 1. SEM image of electrospun nanofibers of (a) pristine PU, (b) PU/CuO with CuO 1%, (c) PU/CuO with CuO 5%, and (d) PU/CuO with CuO 10%. The labels 1 and 2 depict the low and high magnification images.

composite PU nanofibers. Due to the presence of CuO particles in PU polymer solution, the electrical conduction of the solution can be enhanced which further increases the acceleration of jetting polymer solution during the electrospinning process. Therefore, the highly conductive polymer solution gives faster electrospinning. As can be seen from the SEM images, the CuO particles were attached at the periphery of the PU nanofibers. From the SEM data, we have estimated the particles size of CuO in the composite nanofibers. The diameters of the CuO particles are observed to be in the range of 200–500 nm. At the same time, the diameters of the PU/CuO composite nanofibers were almost similar to that of pristine PU nanofibers.

To analyze further the elemental composition of PU/CuO composite nanofibers, SEM-EDX analysis was performed. Fig. 2(a)–(d) shows the SEM-EDX images of the pristine PU and PU/CuO composite nanofibers with different CuO concentrations of 1%, 5% and 10%, respectively. The EDX spectrum clearly confirmed that the PU composite nanofibers consist of copper, oxygen and carbon elements, as shown in Fig. 2. This result confirmed the successful incorporation of CuO particles in PU nanofibers.

XRD is used to investigate the phase structures of the pristine and composite nanofibers. Fig. 3 shows the XRD patterns of pristine and composite PU/CuO nanofibers. The XRD pattern of pristine PU nanofibers showed a broad peak at 20° due to the amorphous nature of the sample. The existence of the prominent XRD patterns corresponding to the CuO particles in the PU phase were observed for the composite nanofibers mats as indexed in the Fig. 3. The intense diffraction peaks at 35°, 38°, 44°, 48°, 64.5° and 78° are corresponding to the (002), (111), (200), (202), (113) and (2 2 0) planes of CuO, which is consistent with the JCPDS data (JCPDS file No. 05-661). The intensity of the diffraction patterns were increased with increasing content of CuO particles, however, the PU/CuO composite nanofibers with CuO content of 1% did not show any significant peaks. This may be due to very low content of CuO particles in the composite nanofibers. No significant diffraction peaks of any other phases or impurities can be detected in the PU/CuO composite nanofibers, which demonstrate the successful incorporation of CuO particles in PU nanofibers. The successful incorporation of CuO particles in PU nanofibers was confirmed by the XRD data which is in good agreement with that of SEM-EDX data.

The bonding configurations of the resultant composite nanofibers were performed by using FT-IR spectroscopy. Fig. 4 shows the FT-IR spectra of pristine and composite nanofibers. These FT-IR spectra illustrate of the interaction between the PU nanofibers containing CuO particles. The characteristic transmittance peaks of the PU films containing metal particles can be assigned as shown in Fig. 4. It can be seen that the characteristic peaks of PU films containing metal

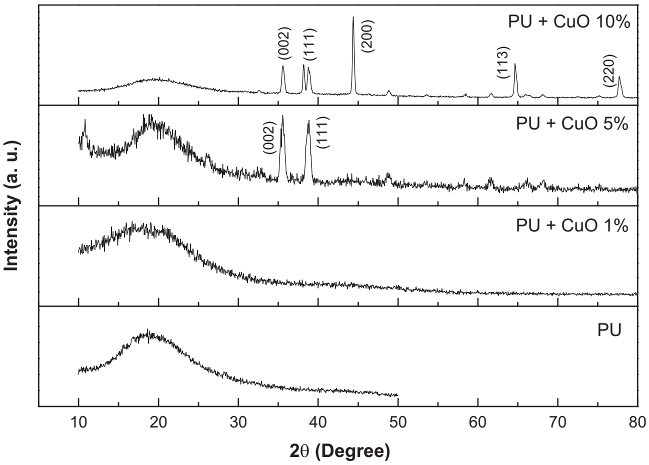

Fig. 3. XRD patterns of PU and PU/CuO composite nanofibers.

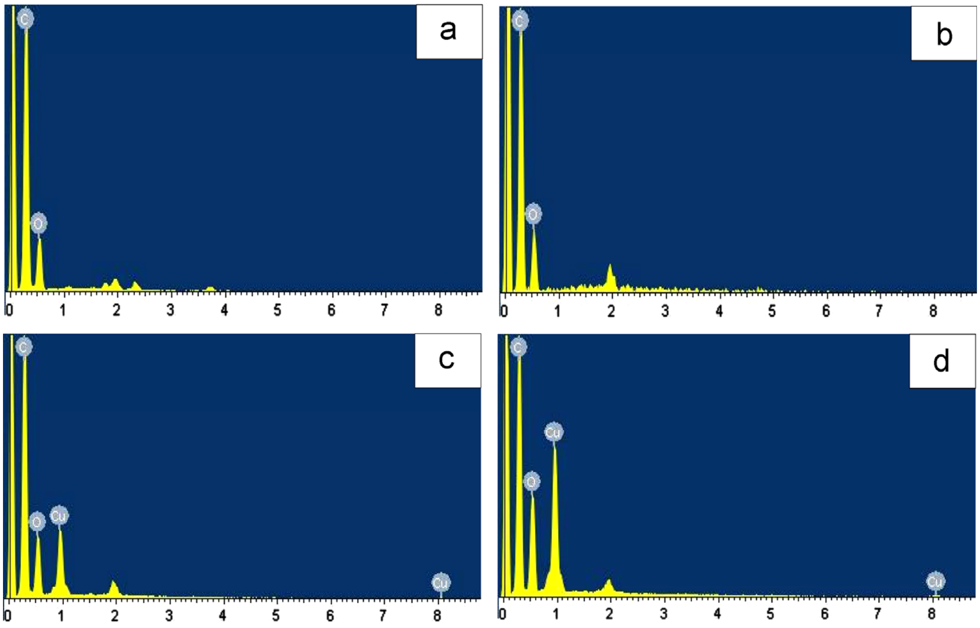

Fig. 2. SEM-EDX image of electrospun nanofibers of (a) pristine PU, (b) PU/CuO with CuO 1%, (c) PU/CuO with CuO 5%, and (d) PU/CuO with CuO 10%.

particles are appeared in the range of 500–1750 cm^{-1}. The FTIR spectroscopy of electrospun composite nanofibers have characteristic transmittance bands at 3240, 2960, 1740, 1530, 1220, 1110 and 777 cm^{-1}, which represents υ (N–H), υ (C–H), υ (C=O), υ (C=C), υ (C–C), υ (C–O), υ (C–H) stretching modes, respectively [33,34]. It was observed that a broad transmittance band centered at 3500 cm^{-1} corresponding to –OH stretch vibration. At the same time, the broad peak between 3200 and 3600 cm^{-1} was increased with increasing content of CuO particles in the composite nanofibers. This is attributed to the increased amount of –OH stretching bonds in the PU/CuO composite nanofibers. Moreover, compared with FT-IR spectrum of pristine PU nanofibers, there was a prominent transmittance peak appeared at 1600 cm^{-1} for the PU/CuO composite nanofibers due to the copper ions and isocyanate group of CuO particles. From these results, we confirm the successful incorporation of CuO particles in PU nanofibers.

Thermal stability of the pristine and PU/CuO composite nanofibers was evaluated using TGA in nitrogen atmosphere. The TGA curves of the pure PU and PU/CuO composite nanofibers are shown in Fig. 5. The onset thermal stability of composite nanofibers was enhanced relative to that of pure PU nanofibers. The onset of decomposition of pristine PU and composite nanofibers were found to be in the range of 200–300 °C. These results indicated that the cations of the copper (e.g., Cu^{2+}) might decrease the thermal stability of PU/CuO composite nanofibers. The effect was attributed to the ability of the cation to form complexes in which the copper atoms were coordinately bonded to urethane group [35]. As expected, the residual weight significantly increases with the incorporation of CuO particles in PU nanofibers. It is noteworthy, to mention that as the amount of CuO particles is increased in the polymer solution, the more residual amount is gained by nanofibers. It was found that the residues of the PU and composite nanofibers at 700 °C were about 8%, 22%, 28%, and 40%, respectively.

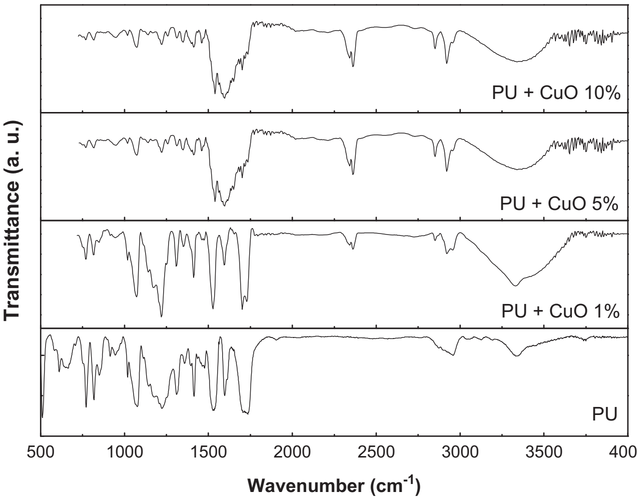

Fig. 4. FT-IR spectra of PU and PU/CuO composite nanofibers.

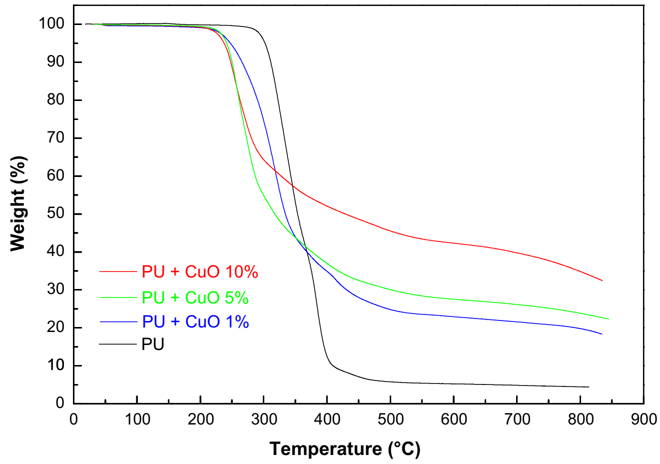

Fig. 5. TGA traces of PU and PU/CuO composite nanofibers.

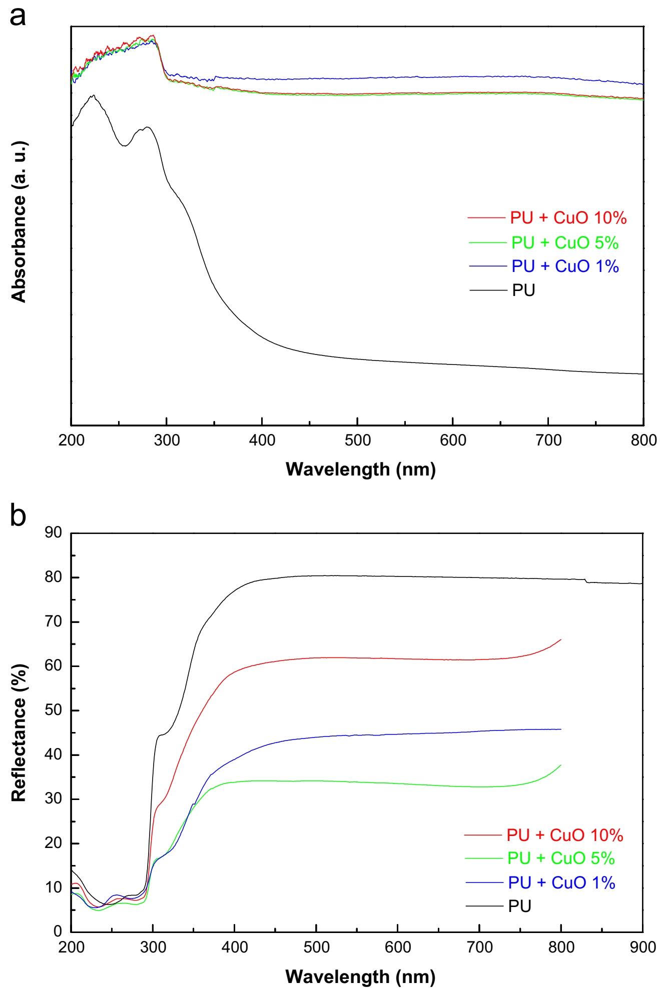

Fig. 6. UV–vis spectra of PU and PU/CuO composite nanofibers (a) absorbance, and (b) reflectance.

Fig. 6 shows the UV–vis spectra of pristine PU and composite nanofibers. As shown from the absorbance spectra in Fig. 6(a), the significant increase in the absorption at a wavelength lower than 300 nm can be observed corresponding to the composite nanofibers containing CuO nanoparticles. The absorbance intensity was increased with the addition of

CuO particles in PU nanofibers, which was attributed to the significant enhancement of light absorption in the visible light region. The respective reflectance spectra of these composite nanofibers are shown in Fig. 6(b). As expected, the reflectance intensity was reduced with the addition of CuO particles in PU nanofibers. It was illustrated that the incorporation of CuO particles in PU nanofibers could effectively block the UV region (200–300 nm). The reflectance was decreased with the addition of CuO particles in PU nanofibers which can be attributed to the effective absorbance of UV emissions by the nanoparticles counterpart homogeneously present in the surfaces of the nanofibers. Such kind of characteristic of these composite nanofibers are of great importance as per technological applications are concerned.

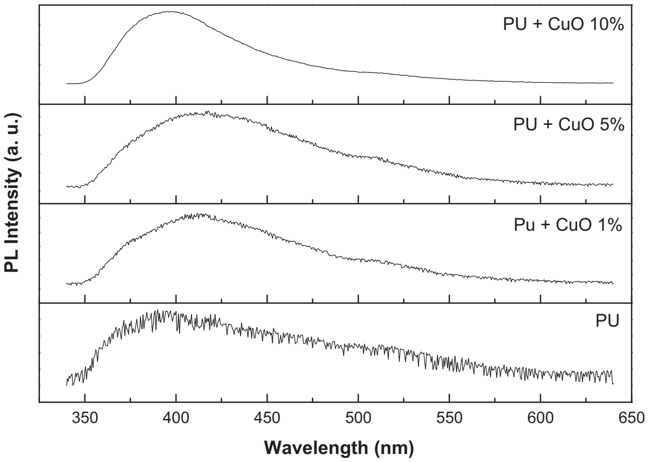

Fig. 7. PL spectra of PU and PU/CuO composite nanofibers.

The luminescence properties of composite nanofibers are useful in understanding the physics of nanostructures and their potential applications in various fields. The PL spectrum of the system is formed as a result of the competition between electron–hole separation, electron–phonon scattering, and electron–hole recombination. Fig. 7 shows the room-temperature PL spectrum of the pristine PU and PU/CuO composite nanofibers. As shown in the PL data, a feeble PL intensity was observed for the pristine PU nanofibers. The PL spectra of the PU/CuO composite nanofibers are dominated by the broad band emission in the range of 350–600 nm. The PL intensity was drastically increased with the incorporation of CuO particles in PU nanofibers. The broad band emission from the PL spectrum at room temperature indicates that the PU/CuO composite nanofibers have good luminescence quality. According to the literature, the intensity of the PL peaks is an indicator for the electrons/hole recombination rate, low intensity indicates low recombination and vice versa [36].

Fig. 8 shows the electrical properties of the composite nanofibers. The *I–V* dependence is typical for a metal–polymer–metal configuration, i.e., it is formed by the characteristics of two point-to-point Schottky diodes. Fig. 8 (a) and (d) shows the *I–V* characteristics of the pristine PU and

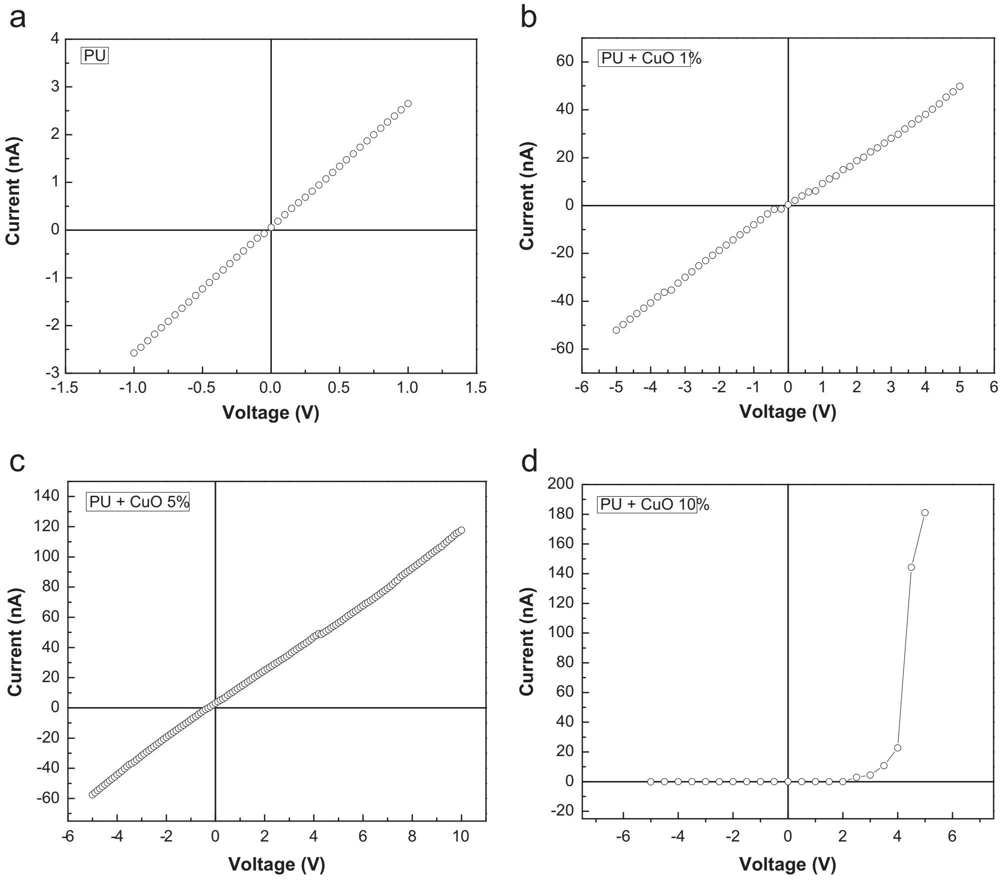

Fig. 8. *I–V* characteristics of nanofibers (a) pristine PU, (b) PU/CuO with CuO 1%, (c) PU/CuO with CuO 5%, and (d) PU/CuO with CuO 10%.

PU/CuO composite nanofibers for the different applied bias voltage ranging between −5 and 10 V, respectively. With the increasing voltage, current is stably increased. It was observed that the pristine PU nanofibers exhibited a current value of 3 nA corresponding to the applied voltage of 1 V. At the same time, when we increased the applied bias beyond 1 V, the current increases abruptly, we could not measure the *I–V* characteristics for the pristine PU nanofibers. The current conduction is unstable. The unstable current characteristic for the pristine PU nanofibers state can be interpreted as the poor conduction nature of the polymer. On the other hand, the CuO particles incorporated composite nanofibers showed quite stable *I–V* characteristics for the large range of applied bias voltages as shown in Fig. 8(b)–(d).

As shown in Fig. 8(a)–(c), the *I–V* characteristics of pristine PU and PU composite nanofibers with CuO content of 1% and 5%, respectively, exhibited almost similar trend of electric conduction behavior except the value of current for the specific applied bias voltage. However, the PU/CuO composite nanofibers with CuO concentration of 10% revealed quite different electric conduction with that of other counterparts studied here. This behavioral appearance of the *I–V* characteristics is attributed to the significant enhancement of carrier concentration in the composite nanofibers. As shown in Fig. 8(d), the measured *I–V* characteristics at room temperature showed a current rectification with a sharp onset voltage of 3.2 V, in the forward bias with relatively negligible leakage currents at the reverse bias. From the *I–V* curve of PU/CuO composite nanofibers, the current is leniently increased with applied voltages as 10 nA at 3 V, 25 nA at 4 V, and 180 nA at 5 V. The enhanced electrical conductivity of these composite nanofibers can readily help the carrier transport in these structures to perform efficient conduction which can be utilized for many technological applications.

4. Conclusions

In summary, we have successfully obtained the CuO particles incorporated PU composite nanofibers by using the electrospinning process. The as-spun PU/CuO composite nanofibers were observed to be smooth with uniform diameters and randomly aligned along their lengths. The resultant composite nanofibers diameters were in the range of 100–300 nm. The surface morphology, optical and electrical characterization of the synthesized PU/CuO composite nanofibers were studied by means of SEM, EDX, XRD, FT-IR, TGA, UV–vis, PL, and *I–V* measurements. The current density and conductivity of the composite PU nanofibers were significantly improved than that of the pristine PU nanofibers. The measured *I–V* characteristics of PU/CuO composite nanofibers with CuO content of 10% showed a current rectification with a sharp onset voltage of 3.2 V, in the forward bias. The significant enhancement of electrical properties of these PU/CuO composite nanofibers can be utilized for quite promising future nanotechnological applications.

Acknowledgments

This research was financially supported by the Ministry of Education, Science Technology (MEST) and National Research Foundation of Korea (NRF) through the Human Resource Training Project for Regional Innovation (2012H1B8A2025931). This work was also supported by the National Research Foundation of Korea (NRF) Grant funded by the Korea government (MEST) (No. 2012R1A2A2A01046086).

References

[1] K.S. Shankar, A.K. Raychaudhuri, Fabrication of nanowires of multicomponent oxides: review of recent advances, Materials Science and Engineering C 25 (2005) 738–751.

[2] C.N.R. Rao, A. Govindaraj, Synthesis of inorganic nanotubes, Advanced Materials 21 (2009) 4208–4233.

[3] S.V.N.T. Kuchibhatla, A.S. Karakoti, D. Bear, S. Seal, One dimensional nanostructures materials, Progress in Materials Science 52 (2007) 699–913.

[4] C.C. Chen, C.C. Yeh, C.H. Chen, M.Y. Yu, H.L Li, J.J. Wu, K.H. Chen, L.C. Chen, J.Y. Peng, Y.F. Chen, Catalytic growth and characterization of gallium nitride nanowires, Journal of American Chemical Society 123 (2001) 2791–2798.

[5] Y. Wu, P. Yang, Germanium nanowire growth via simple vapor transport, Chemical Materials 12 (2000) 605–607.

[6] M.H. Hunag, Y. Wu, H. Feick, N. Tran, E. Weber, P. Yang, Catalytic growth of zinc oxide nanowires by vapor transport, Advanced Materials 13 (2001) 113–116.

[7] W. Han, P. Redlich, F. Ernst, M.R. Uhle, Synthesis of GaN carbon composite nanotubes and GaN nanorods by arc discharge in nitrogen atmosphere, Applied Physics Letters 76 (2000) 652–654.

[8] Y.C. Choi, W.S. Kim, Y.S. Park, S.M. Lee, D.J. Bae, Y.H. Lee, G. S. Park, W.B. Choi, N.S. Lee, J.M. Kim, Catalytic growth of β-Ga2O3 by arc discharge, Advanced Materials 12 (2000) 746–750.

[9] X.F. Duan, C.M. Lieber, General synthesis of compound semiconductor nanowires, Advanced Materials 12 (2000) 298–302.

[10] X. Duan, C.M. Lieber, Laser-assisted catalytic growth of single crystal GaN nanowires, Journal of American Chemical Society 122 (2000) 188–189.

[11] J.Y. Lin, B. Ding, J.Y. Yu, Y. Hsieh, Direct fabrication of highly nanoporous polystyrene fibers via electrospinning, ACS Applied Materials and Interfaces 2 (2010) 521–528.

[12] R. Nirmala, J.W. Jeong, R. Navamathavan, H.Y. Kim, Synthesis and electrical properties of TiO2 nanoparticles embedded in polyamide-6 nanofibers via electrospinning, Nano–Micro Letters 3 (2011) 56–61.

[13] R. Nirmala, B. Woo-il, R. Navamathavan, D. Kalpana, Y.S. Lee, H.Y. Kim, Influence of antimicrobial additives on the formation of rosin nanofibers via electrospinning, Colloids and Surfaces B: Biointerfaces 104 (2013) 262–267.

[14] R. Gopal, S. Kaur, Z. Ma, C. Chan, S. Ramakrishna, T. Matsuura, Electrospun nanofibrous filtration membrane, Journal of Membrane Science 281 (2006) 581–586.

[15] B. Ding, M. Wang, X. Wang, J. Yu, G. Sun, Electrospun nanomaterials for ultrasensitive sensors, Materials Today 13 (2010) 16–27.

[16] U. Ojha, P. Kulkarni, R. Faust, Syntheses and characterization on novel biostable polyisobutylene based thermoplastic polyurethanes, Polymer 50 (2009) 3448–3457.

[17] S. Kidoaki, I.K. Kwon, T. Matsuda, Structural features and mechanical properties of in situ bonded meshes of segmented polyurethane electrospun from mixed solvents, Journal of Biomedical Materials Research B: Applied Biomaterials 76 (2006) 219–229.

[18] B. Cuakmakli, B. Hazer, I.O. Tekin, F.B. Comert, Synthesis and characterization of polymeric soybean oil-g-methyl methacrylate (and n-butyl methacrylate) graft copolymers: biocompatibility and bacterial adhesion, Biomacromolecules 6 (2005) 1750–1758.

[19] H. Deka, N. Karak, R.D. Kalita, A.K. Buragohain, Bio-based thermostable, biodegradable and biocompatible hyperbranched polyurethane/Ag nanocomposites with antimicrobial activity, Polymer Degradation and Stability 95 (2010) 1509–1511.

[20] D.K. Chattopadhaya, K.V.S.N. Raju, Structural engineering of polyurethane coatings for high performance applications, Progress in Polymer Science 32 (2007) 352–418.

[21] X. Liu, Y. Zhao, Z. Liu, D. Wang, J. Wu, D. Xu, Investigation on the interactions between polyurethane and metal chloride, Journal of Molecular Structure 892 (2008) 200–204.

[22] N. Fong, A. Simmons, L.A.P. Warren, Antibacterial polyurethane nanocomposites using chlorhexidine diacetate as an organic modifier, Acta Biomaterialia 6 (2010) 2554–2561.

[23] Y. Choi, R. Nirmala, J.Y. Lee, M. Rahman, S.T. Hong, H.Y. Kim, Antibacterial ciprofloxacin HCl incorporated polyurethane composite nanofibers via electrospinning for biomedical applications, Ceramics International 39 (2013) 4937–4944.

[24] R. Nirmala, K.Y. Nam, R. Navamathavan, S.J. Park, H.Y. Kim, Hydroxyapatite mineralization on the calcium chloride polyurethane nanofibers via biomimetic method, Nanoscale Research Letters 6 (2011) 1–8.

[25] A.S. Lanje, R.S. Ningthoujam, S.J. Sharma, R.K. Vatsa, R.B. Pode, Luminescence properties of $Sn_{1-x}Fe_xO2$ nanoparticles, International Journal of Nanotechnology 7 (2010) 979–988.

[26] S. Anandan, X. Wen, S. Yang, Room temperature growth of CuO nanorod arrays on copper and their application as a cathode in dye-sensitized solar cells, Materials Chemistry and Physics 93 (2005) 35–40.

[27] J. Zhang, J. Liu, Q. Peng, X. Wang, Y. Li, Nearly monodisperse Cu2O and CuO nanoparticles, Chemical Materials 18 (2006) 867–871.

[28] J.B. Reitz, E.I.J. Solomon, Propylene oxidation on copper oxide surfaces: Electronic and geometric contributions to reactivity and selectivity, Journal of American Chemical Society 120 (1998) 11467–11478.

[29] R.V. Kumar, Y. Diamant, A. Gedanken, Sonochemical synthesis and characterization of nanometer-size transition metal oxides from metal acetates, Chemical Materials 12 (2000) 2301–2305.

[30] X. Song, H. Yu, S.J. Sun, Single crystalline CuO nanobelts fabricated by a convenient route, Journal of Colloid Interface Science 289 (2005) 588–591.

[31] H. Hou, Y. Xie, Q. Li, Large-scale synthesis of single crystalline quasi-aligned submicrometer CuO ribbons, Crystal Growth and Design 5 (2005) 201–205.

[32] D. Li, Y.H. Leung, A.B. Djurisic, Z.T. Liu, M.H. Xie, J. Gao, W.K. J. Chan, CuO nanostructures prepared by a chemical method, Journal of Crystal Growth 282 (2005) 105–111.

[33] Z. Jiang, K.J. Yuan, S.F. Li, W.K. Chow, Study of FTIR spectra and thermal analysis of polyurethane, Spectroscopy and Spectral Analysis 26 (2006) 624–628.

[34] R. Chen, C. Huang, Q. Ke, C. He, H. Wang, X. Mo, Preparation and characterization of coaxial electrospun thermoplastic polyurethane/collagen compound nanofibers for tissue engineering applications, Colloids and Surfaces B: Biointerfaces 79 (2010) 315–325.

[35] Y.B. Cai, Q.F. Wei, Q. You, F.L. Huang, L. Song, Y. Hu, Structural, thermal and antibacterial properties of polyacrylonitrile/ferric chloride nanocomposite fibers by electrospinning, International Journal of Polymer Analytical Characterization 15 (2010) 110–128.

[36] J. Liu, J. Li, A. Sedhain, J. Lin, H. Jiang, Structure and photoluminescence study of TiO2 nanoneedle texture along vertically aligned carbon nanofiber arrays, Journal of Physical Chemistry C 112 (2008) 17127–17132.